AD-A186 966 A MODEL OF LIQUID INJECTION IN A REGENERATIVE LIQUID PROPELLANT GUN(U) ARMY BALLISTIC RESEARCH LAB ABERDEEN PROVING GROUND MD W F MORRISON ET AL. JUL 87 1/1

UNCLASSIFIED BRL-TR-2851 F/G 19/1 NL

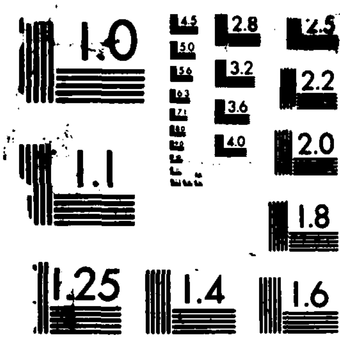

MICROCOPY RESOLUTION TEST CHART
NATIONAL BUREAU OF STANDARDS-1963-A

DTIC FILE COPY

AD-F300 982

(12)

AD

AD-A186 966

TECHNICAL REPORT BRL-TR-2851

A MODEL OF LIQUID INJECTION IN A REGENERATIVE LIQUID PROPELLANT GUN

WALTER F. MORRISON
GLORIA P. WREN

DTIC
ELECTE
NOV 2 5 1987
S D
D

JULY 1987

APPROVED FOR PUBLIC RELEASE; DISTRIBUTION UNLIMITED

US ARMY BALLISTIC RESEARCH LABORATORY
ABERDEEN PROVING GROUND, MARYLAND

87 11 18 011

UNCLASSIFIED

SECURITY CLASSIFICATION OF THIS PAGE

ADA186966

REPORT DOCUMENTATION PAGE

Form Approved
OMB No 0704-0188
Exp. Date Jun 30, 1986

1a. REPORT SECURITY CLASSIFICATION: Unclassified	1b. RESTRICTIVE MARKINGS
2a. SECURITY CLASSIFICATION AUTHORITY	3. DISTRIBUTION/AVAILABILITY OF REPORT
2b. DECLASSIFICATION/DOWNGRADING SCHEDULE	
4. PERFORMING ORGANIZATION REPORT NUMBER(S): BRL-TR-2851	5. MONITORING ORGANIZATION REPORT NUMBER(S)
6a. NAME OF PERFORMING ORGANIZATION: US Army Ballistic Resch Lab; 6b. OFFICE SYMBOL (If applicable): SLCBR-IB	7a. NAME OF MONITORING ORGANIZATION
6c. ADDRESS (City, State, and ZIP Code): Aberdeen Proving Ground, MD 21005-5066	7b. ADDRESS (City, State, and ZIP Code)
8a. NAME OF FUNDING/SPONSORING ORGANIZATION; 8b. OFFICE SYMBOL (If applicable)	9. PROCUREMENT INSTRUMENT IDENTIFICATION NUMBER
8c. ADDRESS (City, State, and ZIP Code)	10. SOURCE OF FUNDING NUMBERS: PROGRAM ELEMENT NO. / PROJECT NO. / TASK NO. / WORK UNIT ACCESSION NO

11. TITLE (Include Security Classification)

A MODEL OF LIQUID INJECTION IN A REGENERATIVE LIQUID PROPELLANT GUN

12. PERSONAL AUTHOR(S)

Morrison, Walter F. and Wren, Gloria P.

13a. TYPE OF REPORT	13b. TIME COVERED	14. DATE OF REPORT (Year, Month, Day)	15. PAGE COUNT
TR	FROM ____ TO ____		

16. SUPPLEMENTARY NOTATION

17. COSATI CODES			18. SUBJECT TERMS (Continue on reverse if necessary and identify by block number)
FIELD	GROUP	SUB-GROUP	

19. ABSTRACT (Continue on reverse if necessary and identify by block number)

A lumped parameter model of liquid injection in a regenerative liquid propellant gun is developed. A set of ordinary differential equations is presented which account for (1) the coupling between piston motion and liquid injection and (2) the inertia of the liquid in the reservoir. Results of the simulation are presented and compared to experimental data from a 30-mm RLPG test fixture.

20. DISTRIBUTION/AVAILABILITY OF ABSTRACT: ☒ UNCLASSIFIED/UNLIMITED ☐ SAME AS RPT ☐ DTIC USERS	21. ABSTRACT SECURITY CLASSIFICATION: Unclassified
22a. NAME OF RESPONSIBLE INDIVIDUAL: Walter F. Morrison	22b. TELEPHONE (Include Area Code): 301-278-6189; 22c. OFFICE SYMBOL: SLCBR-IB-B

DD FORM 1473, 84 MAR

83 APR edition may be used until exhausted
All other editions are obsolete

SECURITY CLASSIFICATION OF THIS PAGE
UNCLASSIFIED

TABLE OF CONTENTS

DTIC
COPY
INSPECTED

Accesion For
NTIS CRA&I
DTIC TAB
A-1

LIST OF FIGURES

I. INTRODUCTION

The interior ballistic process in the regenerative liquid propellant gun is primarily controlled by the rate of injection of the liquid propellant, and, thus by the motion of the regenerative piston. In the interior ballistic models developed to date by Gough,[1 2] Coffee,[3] Cushman[4] and Bulman[5] the equations of motion for the regenerative piston describe only the pressure and friction forces. These models, in general, neglect any direct coupling between piston motion and liquid injection. The formulation of Cushman,[4] which has been discussed by Gough,[1] is an exception.

Using Gough's[1] approach, the equations of motion for the piston and the liquid can be written in the form,

$$\dot{u}_p = 1/M_p \left\{ P_3 A_p - \bar{P} A_R + A_3 \left[1 - A_3/A_L - 1/2\, C_D^{\,2}\right] {}_L\, v_3^{\,2} \right\}, \tag{1}$$

$$\dot{v}_3 = 1/\rho_L l_H \{\bar{P} - P_3 - \rho_L v_3^{\,2}/2C_D^{\,2}\}, \tag{2}$$

where the C_D is the discharge coefficient,

$$C_D = \left[1 - \left(\frac{A_3}{A_L}\right)^2 + (1/\psi - 1)^2 + \frac{0.3164 l_H}{Re^{1/4}\, D_H}\right]^{-1/2}. \tag{3}$$

The first two terms on the right hand side of the equation account for the kinetic energy of the liquid exiting and approaching the injector, respectively. The term involving ψ is an injector entrance loss, as described by Kaufmann,[6] and the last term is the usual Blasius correlation for the pressure head loss due to friction in turbulent pipe flow.

As noted, the more usual formulations of the equations for piston motion and liquid injection neglect coupling between the physical processes. In general, the acceleration of the liquid through the injector is also neglected, resulting in equations of the form,

$$\dot{u}_p = 1/M_p \{P_3 A_p - \bar{P} A_R\} , \quad (4)$$

$$v_3 = C_D [2 (\bar{P} - P_3)/\rho_L]^{1/2} . \quad (5)$$

While it is acknowledged that the development of the above equations involve numerous approximations, until recently it has appeared that such simple models were adequate to describe piston motion and liquid injection in the regenerative gun. However, Pate[7] has reported values of the discharge coefficient in cold flow experiments in a regenerative LP fixture which significantly exceed those predicted using equation 3. In addition, Coffee[8] has reported a discharge coefficient derived from regenerative gun firing data which not only exceeds the predicted value, but also is highly transient in nature. Finally, Rizk and Edelman[9] have reported values of the discharge coefficient, obtained from a two dimensional simulation of the cold flow experiment of Pate, which are in agreement with experimental data.

The objective of this work is to investigate liquid injection in the regenerative liquid propellant gun, within the context of a lumped parameter model. This requires the development of a set of ordinary differential equations, similar to 1 and 2, but which more accurately account for; (1) the coupling between piston motion and liquid injection and (2) the inertia of the liquid in the reservoir. This report describes the progress to date in this effort. A general mathematical model describing the process has been developed. Results of the simulation are presented and compared to experimental data from a 30mm RLPG test fixture.

The governing equations have been coded in FORTRAN for the IBM PC-AT, using the Adams method with functional iteration from the IMSL Library, DGEAR.

II. EQUATIONS OF MOTION

The equations of motion are written for the control volume containing the regenerative piston and the liquid propellant reservoir, as shown in Fig. 1.

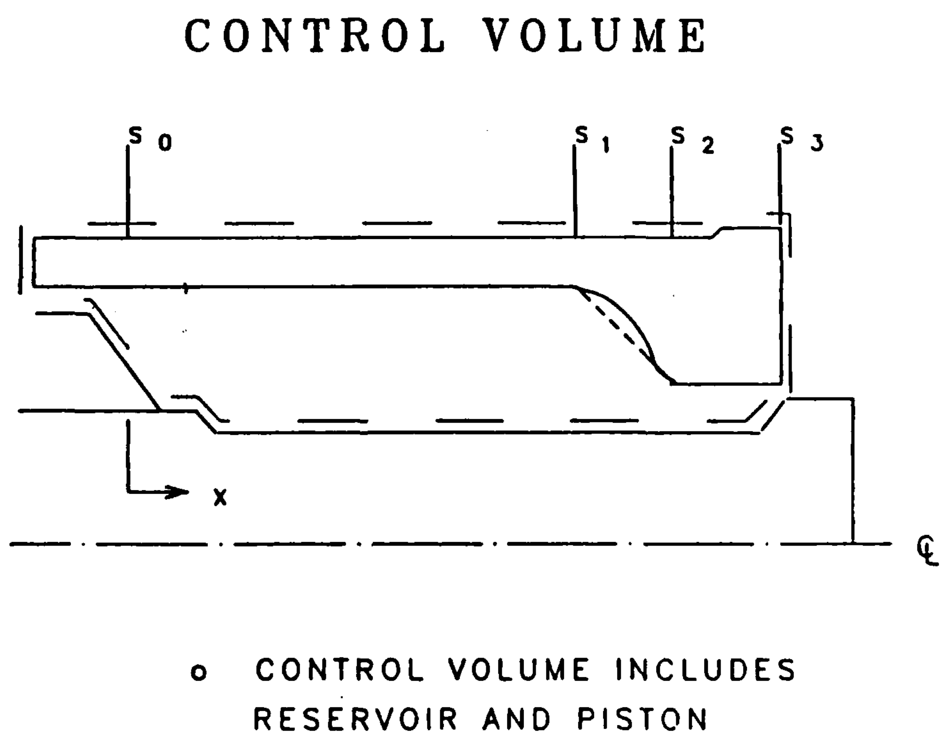

Figure 1. Control Volume

The contours of the piston and the reservoir are approximated by straight line segments as indicated. The center bolt and transducer bolt are fixed in the reference frame of the chamber. The origin of our coordinate system is fixed at the rear (left hand) end of the reservoir, and x is the coordinate along the bolt with x_1, x_2, and x_3 the coordinates of fixed positions on the bolt as shown. The piston moves rearward with a velocity u_p, and the points s_1, s_2, and s_3 are the coordinates of fixed stations on the inner contour of the piston with respect to the origin, as shown, such that these coordinates vary with time as the piston is displaced to the left. Note that the right hand face of the control volume is attached to the chamber face of the piston (s_3) such that the control volume also varies with time.

The equations of motion are written in the reference frame of the bolt (chamber). The momentum equation for the control volume $[0,s_3]$ is

$$M_p \dot{\vec{u}}_p + \frac{\partial}{\partial t} \int_{cv} \vec{v}\rho_L dV + \int_{cs} \vec{v}\rho_L \vec{v} \, d\vec{A} = -\int_{cs} P \, d\vec{A} \tag{6}$$

where M_p is the mass of the piston and $d\vec{A}$ is the outward directed normal from the element of control surface. Then,

$$-M_p \dot{u}_p \hat{i} + \frac{\partial}{\partial t} \left[\int_0^{s_3} \rho_L \, vA \, dx \right] \hat{i} + \rho_L v_3^2 A_3 \hat{i} =$$

$$[P_O A_L + P_{CF} A_S - P_3 (A_p + A_3)] \hat{i} \tag{7}$$

where the control volume extends to include the piston shaft and P_{CF} represents the pressure of a control fluid on the area of the piston shaft, A_S. We will ignore this term in this paper, and write the momentum equation for the control volume as

$$M_p \dot{u}_p - \frac{\partial}{\partial t}\left[\int_0^{s_3} \rho_L v A \, dx\right]$$

$$= P_3 (A_p + A_3) - P_0 A_L + \rho_L v_3^2 A_3 \, . \tag{8}$$

The unsteady Bernoulli equation is,

$$\int_0^{s_3} \dot{v} \, dx = \frac{1}{\rho_L} (P_0 - P_3) - \frac{1}{2} v_3^2 - h_f - h_f' \tag{9}$$

where h_f is the headloss due to friction, and h_f' is an entrance loss.

The integrals of interest are then,

$$\int_0^{s_3} \dot{v}(x,t) \, dx \quad \text{and} \quad \frac{\partial}{\partial t} \int_0^{s_3} \rho_L(x,t) \, v(x,t) \, A(x,t) \, dx \, .$$

In order to evaluate these integrals, we require $\rho(x,t)$ and $v(x,t)$.

III. LAGRANGE APPROXIMATION WITH AREA CHANGE

The equations of motion for the fluid are

$$\frac{\partial}{\partial t} (\rho_L A) + \frac{\partial}{\partial x} (\rho_L v A) = 0 \tag{10}$$

$$\frac{\partial}{\partial t} (\rho_L v A) + \frac{\partial}{\partial x} (\rho_L v^2 A) = - A \frac{\partial P}{\partial x} \tag{11}$$

The position of a fixed point j on the piston in the coordinate system attached to the bolt (or chamber) is defined as $s_j(t)$ where

$$\dot{s}_j(t) = - u_p(t) \tag{12}$$

and

$$\left(\frac{\partial s}{\partial x} \right)_t = 1 \; . \tag{13}$$

Approximating the contour on the inner surface of the piston by the dashed straight line above, we can express the radius of the piston as measured from the center line as

$$R(x,t) = \{R_1 + \frac{(R_2 - R_1)}{(s_2 - s_1)} [x - s_1] \; [1 - H(s_1 - x)]\} \; H\,(s_2 - x)$$

$$+ R_2 \; [1 - H(s_2 - x)] \; H(s_3 - x) \tag{14}$$

where x indicates the position on the bolt, R_1 indicates the radius of the piston at s_1 and R_2 is the radius of the piston at s_2. H(x) is the Heaviside function defined as H(x) = 0 for x<0 and H(x) = 1 for x>=0. The radius of the inner surface of the piston at a position x is time dependent since the piston is moving.

Similarly, the radius of the bolt at any position x on the bolt can be expressed

$$r_b(x) = \{r_b + \frac{(r_2 - r_1)}{(x_2 - x_1)} [x - x_1][1 - H(x_1 - x)]\} H(x_2 - x)$$

$$+ r_2 [1 - H(x_2 - x)] H(x_3 - x) . \tag{15}$$

The cross-sectional area of the liquid is then given by

$$A(x,t) = \pi [R^2(x,t) - r_b^2(x)] \tag{16}$$

and the volume of the liquid is

$$V(x,t) = \int_0^{s(x,t)} A(x',t)\, dx' . \tag{17}$$

Then it can be shown that

$$\dot{A}(x,t) = u_p \frac{\partial A(x,t)}{\partial x} \tag{18}$$

and

$$\dot{V}_R = - u_p (A_R + A_3) . \tag{19}$$

Returning now to equation (10), and assuming

$$\partial\rho_L/\partial x = 0$$

We have,

$$A \frac{1}{\rho_L} \frac{\partial \rho_L}{\partial t} = - \frac{\partial A}{\partial t} - \frac{\partial vA}{\partial x} \, . \tag{20}$$

Now,

$$\frac{\partial \rho_L}{\partial t} = \frac{\partial}{\partial t} \left[\frac{m_L}{V_R} \right] = \frac{\dot{m}_L}{V_R} - \frac{m_L \dot{V}_R}{V_R^2}$$

$$= \frac{1}{V_R} \left[[-\rho_L v_3 A_3 - \rho_L u_p A_3] - [-\rho_L u_p (A_R + A_3)] \right]$$

where

$\rho v_3 A_3$ is the mass flux through the orifice with respect to the bolt, and

$\rho u_p A_3$ is the additional mass flux into the chamber due to piston motion.

Then,

$$\frac{1}{\rho_L} \frac{\partial \rho_L}{\partial t} = - \frac{v_3 A_3 - u_p A_R}{V_R} \, . \tag{21}$$

Now using (18) and (21), equation (20) becomes

$$\frac{\partial vA}{\partial x} = - u_p \frac{\partial A}{\partial x} + \frac{v_3 A_3 - u_p A_R}{V_R} A \, . \tag{22}$$

Integrating on $x<s_3$, and noting that $v(0,t) = 0$, we have

$$v(x,t)\ A(x,t) = -\ u_p A(x,t)\ \Big|_0^x + [v_3A_3 - u_pA_R]\ \frac{V(x,t)}{V_R}\ \Big|_0^x \tag{23}$$

or

$$v(x,t)\ A(x,t) = u_p[A_L - A(x,t)] + [v_3A_3 - u_pA_R]\ \frac{V(x,t)}{V_R} \tag{24}$$

where $A_L = A_R + A_3$.

Using equation (10) in (11) we obtain

$$\rho_L A\ \frac{\partial v}{\partial t} + \rho_L Av\ \frac{\partial v}{\partial x} = -\ A\ \frac{\partial \rho_L}{\partial x}\ , \tag{25}$$

or, integrating on $x<s_3$

$$P(x,t) = P_0(t) - \frac{1}{2}\ \rho_L v^2(x,t) - \rho_L \int_0^x \dot{v}(x,t)\ dx'\ . \tag{26}$$

The objective is to define a space-mean pressure using the pressure distribution in the reservoir. While it appears feasible to simply substitute equation (24) in (26) and complete the required integrations, the results would be complex. Instead, we define the space-mean pressure on $[0,s_1]$ as

$$\overline{P}(t) = \frac{1}{l_{01}(t)} \int_0^{s_1} P(x,t)\ dx \tag{27}$$

where $l_{01}(t)$ is the length of the reservoir from 0 to s_1 at time t and the velocity $v(x,t)$ on $[0,s_1]$ is

$$v(x,t) = \left[\frac{v_3A_3 - u_pA_R}{V_R}\right] x \quad , \quad [0,s_1] \; . \tag{28}$$

Substituting, we obtain

$$P(x,t) = P_O(t) - \frac{1}{2}\,\rho_L x^2 \left\{ \left[\frac{v_3A_3 - u_pA_R}{V_R}\right]^2 + \frac{\partial}{\partial t}\left[\frac{v_3A_3 - u_pA_R}{V_R}\right] \right\} . \tag{29}$$

The term in brackets can be rewritten as,

$$\frac{\dot v_3A_3 - \dot u_pA_R}{V_R} + \frac{u_p\,A_L\,(v_3A_3 - u_p\,A_R)}{V_R^{\,2}} + \frac{(v_3\,A_3 - u_p\,A_R)^2}{V_R^{\,2}}$$

$$= \frac{\dot v_3\,A_3 - \dot u_p\,A_R}{V_R} + \frac{(u_p + v_3)\,A_3\,(v_3\,A_3 - u_p\,A_R)}{V_R^{\,2}} \; . \tag{30}$$

Using equations (29) and (30) in (27) we have

$$P_O(t) = \bar P(t) + \frac{1}{6}\, l_{01}^{2}(t) \left\{ \frac{\dot v_3A_3 - \dot u_pA_R}{V_R} + \frac{(u_p + v_3)A_3(v_3A_3 - u_pA_R)}{V_R^{\,2}} \right\} . \tag{31}$$

IV. EVALUATION OF INTEGRALS

Consider first $\int_0^{s_3} \dot v(x,t)\,dx$

Equation (24) can be rewritten in the form,

$$v(x,t) = u_p \left[\frac{A_L}{A(x)} - 1 \right] + \frac{[v_3 A_3 - u_p A_R]}{A_L} \frac{A_L}{A(x)} \frac{V(x)}{V_R} . \tag{32}$$

Integrating, we have

$$\int_0^{s_3} v(x,t)\, dx = u_p \int_0^{s_3} \left[\frac{A_L}{A(x)} - 1 \right] dx$$

$$+ \frac{[v_3 A_3 - u_p A_R]}{A_L} \frac{A_L}{V_R} \int_0^{s_3} \frac{V(x)}{A(x)}\, dx . \tag{33}$$

We now define three effective lengths,

$$L^1_{03}(t) = \frac{1}{V_R} \int_0^{s_3} V(x)\, dx \tag{34}$$

$$L^2_{03}(t) = \frac{A_L}{V_R} \int_0^{s_3} \frac{V(x)}{A(x)}\, dx \tag{35}$$

$$L^3_{03}\ (t) = A_L \int_0^{s_3} \frac{dx}{A(x)} \tag{36}$$

and let $l_{03}(t)$ represent the time-dependent length of the reservoir from the rear of the liquid chamber to the exit at the vent.

Rewriting the integral, we have

$$\int_0^{s_3} v(x,t)\,dx = u_p\,[L_{03}^3(t) - l_{03}(t)] + \frac{[v_3A_3 - u_pA_R]}{A_L}\,L_{03}^2(t)\ . \qquad (37)$$

We now note that

$$\int_0^{s_3} \dot{v}(x,t)\,dx = \frac{\partial}{\partial t}\int_0^{s_3} v(x,t)\,dx + u_p\,v_3 . \qquad (38)$$

Using equation (37), we have

$$\int_0^{s_3} \dot{v}(x,t)\,dx = \dot{u}_p\,[L_{03}^3(t) - l_{03}(t) - \frac{A_R}{A_L}\,L_{03}^2(t)]$$

$$+ \dot{v}_3\,\frac{A_3}{A_L}\,L_{03}^2(t) + u_p v_3 + \frac{[v_3A_3 - u_pA_R]}{A_L}\,\dot{L}_{03}^2(t) \qquad (39)$$

where we have used the facts that

$\dot{L}_{03}^3(t) = \dot{l}_{01}(t) = -\,u_p$, and $\dot{l}_{03}(t) = -\,u_p$, and where we have assumed $\dot{A}_3 = 0$

since the vent area is variable only over the slant section of the bolt.

Consider now $\frac{\partial}{\partial t}\int_0^{s_3} \rho_L vA\,dx$.

Recalling that $d\rho_L/dx = 0$, and substituting equation (24), we have

$$\rho_L \int_0^{s_3} vA(x,t)\, dx = \frac{\partial}{\partial t} \{\rho_L [u_p A_L \, (l_{03}(t) - \frac{V_R}{A_L})$$

$$+ (v_3 A_3 - u_p A_R)\, L^1_{03}(t)]\} \tag{40}$$

giving us,

$$\frac{\partial}{\partial t} \rho \int_0^{s_3} vA(x,t)\, dx = \dot{u}_p \, \{\rho_L A_L \, (l_{03}(t) - \frac{V_R}{A_L}) - \rho_L A_R \, L^1_{01}(t)\}$$

$$+ \dot{v}_3 \, [\rho_L A_3 \, L^1_{03}(t)] + \rho_L \, (v_3 A_3 - u_p A_R)\, \dot{L}^1_{03}(t)$$

$$+ \frac{\partial \rho_L}{\partial t} \int_0^{s_3} vA \, dx \, . \tag{41}$$

V. EVALUATION OF EFFECTIVE LENGTHS

In order to simplify the effective length integrals we assume that the bolt is straight and consider the area change of the piston only. Then,

$$L^1_{03}(t) = \frac{l^2_{01}(t)\, A_L}{2V_R} + \frac{1}{V_R} \{l_{12} \, [l_{01}(t)\, A_L]$$

$$+ \frac{\pi}{M^2} \, [R_1(R_1 - R_2) \, (\frac{1}{3}R_1{}^2 - r_b{}^2) + \frac{1}{2} r_b{}^2 \, (R_1{}^2 - R_2{}^2) - \frac{1}{12} \, (R_1{}^4 - R_2{}^4)]\}$$

$$+ \frac{1}{V_R} \{l_H \, [l_{01}(t)\, A_L + V_{12}] + [\, \frac{1}{2} A_3 \, (l^2_{13} - l^2_{12}) \,]\} \tag{42}$$

$$L_{03}^2(t) = \{ \frac{1}{2} l_{01}^2(t) \frac{A_L}{V_R} \} + \frac{A_L}{V_R} \Bigg[\{ \frac{l_{01}(t) A_L}{\pi M}$$

$$+ \frac{R_1((1/3) R_1^2 - r_b^2)}{M^2} \} \frac{1}{2r_b} [\ln (\frac{A_L}{A_3}) - 2 \ln (\frac{R_1 + r_b}{R_2 + r_b})]$$

$$+ \frac{r_b^2}{3M^2} \ln (\frac{A_L}{A_3}) - \frac{R_1^2 - R_2^2}{6M^2} \Bigg] + \frac{A_L}{V_R} \Bigg[\frac{l_{23}[l_{01}(t) A_L + V_{12}]}{A_3}$$

$$+ \frac{1}{2} (l_{13}^2 - l_{12}^2) + l_{01}(t) l_{23} \Bigg] \qquad (43)$$

$$L_{03}^3(t) = l_{01}(t) + \frac{A_L}{2\pi r_b M} [\ln (\frac{A_L}{A_3})] - 2 \ln (\frac{R_1 + r_b}{R_2 + r_b})]$$

$$+ l_{23} \frac{A_L}{A_3} \qquad (44)$$

$$L_{13}^3(t) = L_{03}^3(t) - l_{01}(t) \qquad (45)$$

where $M = (R_1 - R_2) / (x_2 - x_1)$.

While the effective lengths above are all time dependent, the time derivatives do not contribute terms in $\dot{u}_\rho$ or $\dot{v}_3$.

VI. PISTON AND LIQUID ACCELERATION

Substituting (31), (39) and (41) into equations (8) and (9) we have

$$\dot{u}_p \left[M_p + \rho_L A_R L_{03}^1(t) - \rho_L A_L \left(l_{03}(t) - \frac{V_R}{A_L}\right) - \frac{\rho_L A_R A_L l_{01}^2(t)}{6 V_R}\right]$$

$$- \dot{v}_3 \left[\rho_L A_3 L_{03}^1(t) - \frac{\rho_L A_3 A_L l_{01}^2(t)}{6 V_R}\right] =$$

$$P_3 (A_p + A_3) - \bar{P} A_L + \rho_L v_3^2 A_3$$

$$- \frac{1}{6} \rho_L A_L l_{01}^2(t) + \frac{(u_p + v_3) A_3 (v_3 A_3 - u_p A_R)}{V_R^2}$$

$$+ \rho_L (v_3 A_3 - u_p A_R) \dot{L}_{03}^1(t) + \frac{\partial \rho_L}{\partial t} \int_0^{s_3} vA(x,t)\, dx \qquad (46)$$

and

$$\dot{u}_p \left[L_{03}^3(t) - l_{03}(t) - \frac{A_R}{A_L} L_{03}^2(t) + \frac{l_{01}^2(t) A_R}{6 V_R}\right]$$

$$+ \dot{v}_3 \left[\frac{A_3}{A_L} L_{03}^2(t) - \frac{A_3 l_{01}^2(t)}{6 V_R}\right] =$$

$$\frac{1}{\rho_L}(\bar{P} - P_3) - \frac{1}{2} v_3^2 - h_f - h_{f'} + \frac{1}{6} l_{01}^2(t) \left[\frac{(u_p + v_3) A_3 (v_3 A_3 - u_p A_R)}{V_R^2}\right]$$

$$- u_p v_3 - \frac{v_3 A_3 - u_p A_R}{A_L} \dot{L}_{03}^2(t) \, . \qquad (47)$$

Now defining G and F as the right hand sides of (46) and (47), we have

$$\dot{u}_p \left[M_p + \rho_L A_R L^1_{03}(t) - \rho_L A_L \left(l_{03}(t) - \frac{V_R}{A_L}\right) - \frac{\rho_L A_R A_L l^2_{01}(t)}{6V_R}\right]$$

$$- \dot{v}_3 \left[\rho_L A_3 L^1_{03}(t) - \frac{\rho_L A_3 A_L l^2_{01}(t)}{6V_R}\right] = G \tag{48}$$

and

$$\dot{u}_p \left[L^3_{03}(t) - l_{03}(t) - \frac{A_R}{A_L} L^2_{03}(t) + \frac{l^2_{01}(t) A_R}{6V_R}\right]$$

$$+ \dot{v}_3 \left[\frac{A_3}{A_L} L^2_{03}(t) - \frac{A_3 l^2_{01}(t)}{6V_R}\right] = F , \tag{49}$$

and further defining

$$m_{eff} = \left[\rho_L A_3 L^1_{03}(t) - \frac{\rho_L A_R A_L l^2_{01}(t)}{6V_R}\right] \tag{50}$$

$$l_{eff} = \left[\frac{A_3}{A_L} L^2_{03}(t) - \frac{A_3 l^2_{01}(t)}{6V_R}\right] \tag{51}$$

$$M_{eff} = M_p + \frac{A_R}{A_3} m_{eff} - \rho_L A_L \left[l_{03}(t) - \frac{V_R}{A_L}\right] \tag{52}$$

$$L_{eff} = l_{03}(t) - L^3_{03}(t) + \frac{A_R}{A_3} l_{eff} \tag{53}$$

we can rewrite equations (48) and (49),

$$\dot{u}_p M_{eff} - \dot{v}_3 m_{eff} = G \tag{54}$$

$$\dot{v}_3 l_{eff} - \dot{u}_p L_{eff} = F . \tag{55}$$

Solving for $\dot{u}_p$ and $\dot{v}_3$, and defining

$$M_p' = M_p - \rho_L A_L [l_{03}(t) - \frac{V_R}{A_L}] - m_{eff} \frac{l_{01}(t) - L^3_{03}(t)}{l_{eff}} \tag{56}$$

$$F' = \frac{1}{l_{eff}} F \tag{57}$$

we have

$$\dot{u}_p = \frac{1}{M_p'} G + \frac{m_{eff}}{M_p'} F' \tag{58}$$

$$\dot{v}_3 = F' [1 + \frac{L_{eff}}{l_{eff}} \frac{m_{eff}}{M_p'}] + \frac{L_{eff}}{l_{eff}} \frac{1}{M_p'} G . \tag{59}$$

VII. ADDITIONAL EQUATIONS

To complete the description of the liquid chamber we need equations for the piston position and mass flux.

$$\dot{x}_p = u_p \tag{60}$$

$$\dot{m}_L = - \rho_L A_3 V_3 \ . \qquad (61)$$

The equation of state for liquid monopropellants is

$$P_R = P_O + \frac{K_1}{K_2} \left[\left(\frac{\rho_L}{\rho_O}\right)^{K_2} - 1 \right] \qquad (62)$$

where the density is determined by

$$\rho_L = \frac{m_L}{V_R} \ . \qquad (63)$$

The governing equations for the lumped parameter model, equations (58-63), are a system of first order differential equations, which have been solved in standard FORTAN using the Adams method with functional iteration in the IMSL library DGEAR on an IBM PC-AT. The chamber pressure boundary condition is specified as an input, using the experimentally measured chamber pressure from a 2/3 charge firing of a Concept VI regenerative liquid propellant gun test fixture at the Ballistic Research Laboratory.

VIII. RESULTS AND DISCUSSION

Experimental chamber and liquid pressures, and piston displacement from the 2/3 charge firing used in specifying the chamber pressure boundary condition are presented in Fig. 2. The zero in time has been chosen as the time at which the pressure begins to rise in the combustion chamber due to the influx of gas from the igniter.

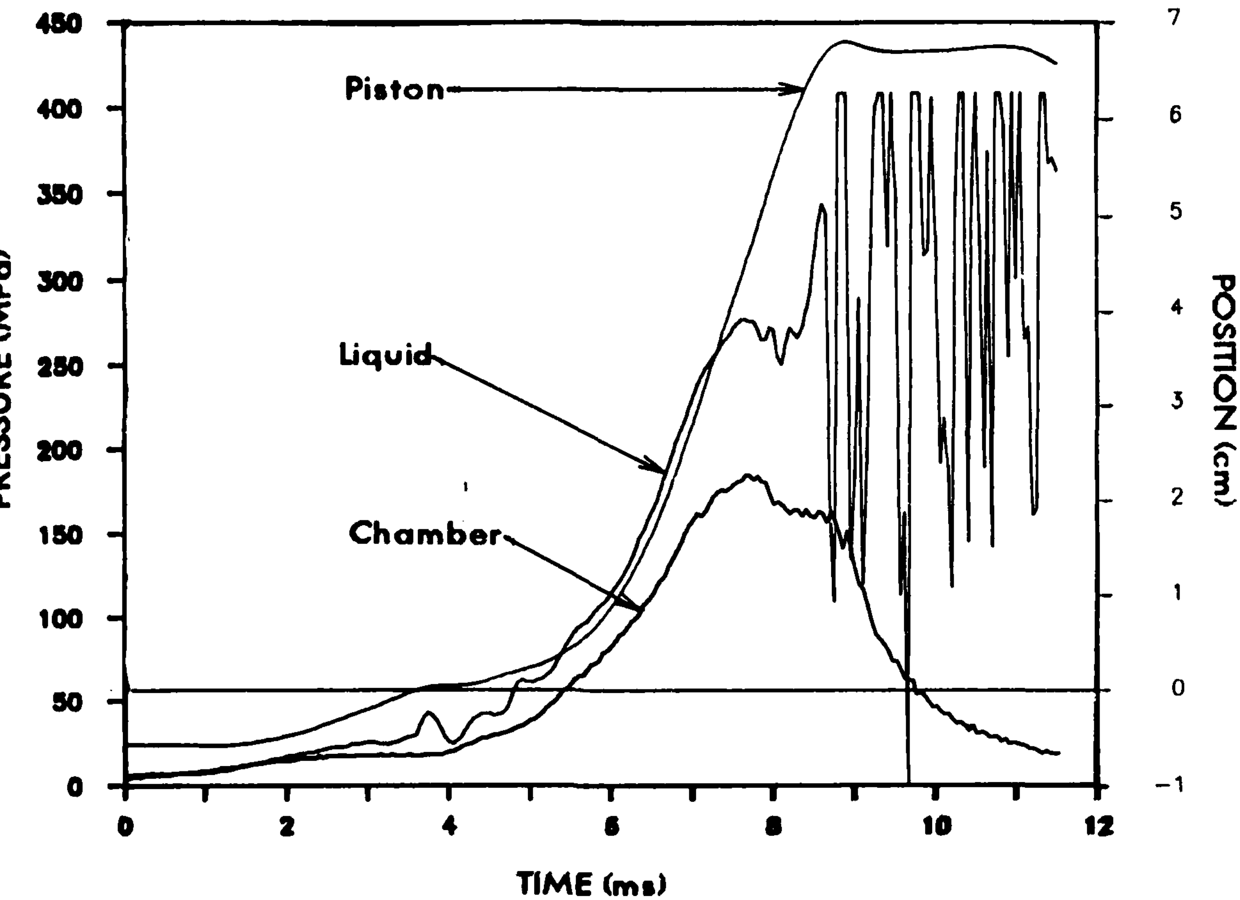

Figure 2. Experimental Chamber Pressure, Liquid Pressure, Piston Displacement

The piston begins to move at about 1.25 ms, travels about 0.55 cm and abruptly stops at about 3.5 ms, hestitates briefly and then again accelerates and smoothly completes its stroke. This interrupted piston travel is a characteristic of the Concept VI RLPG. In order to permit the piston to clear the seal on the nose of the center bolt, the piston, liquid reservoir, and transducer block initially move rearward approximately 0.55 cm against a set of Belleville springs. When the springs are fully compressed, the transducer block abruptly stops, as does the reservoir and piston. The piston then accelerates rearward again as liquid injection begins, and completes its stroke.

The chamber pressure rises steadily to about 20 MPa in about 2.4 ms, and then maintains that value until about 4 ms when liquid propellant combustion begins. The chamber pressure then rises smoothly to its maximum value, drops slightly as the piston reaches the rear taper of the bolt at about 8 ms, and then drops sharply at burnout as the piston completes its stoke at about 9 ms.

The propellant in the reservoir is much stiffer than the combustion gases, and thus reflects the abrupt variations in piston motion. As the Belleville springs begin to compress, a small oscillation in liquid pressure is observed at about 3 ms. When the transducer block suddenly stops at about 3.5 ms, the momentum of the piston is absorbed by the liquid, producing the relatively large hydraulic pressure oscillations from 3.5 ms to 5.0 ms. Initially these oscillations are undamped; however, as the injection area opens, the oscillations are rapidly damped. Similarly, as the piston reaches the rear taper, which reduces the liquid injection area, the liquid pressure rises sharply as the piston is decelerated. The liquid reservoir gage fails just as damping begins at about 8 ms.

No attempt has been made here to simulate the motion of the transducer block against Belleville springs. Instead, the zero in time is chosen to be the point at which the piston stops due to completion of transducer block motion, and the initial conditions for the solution of the ordinary differential equations are then taken from experimental data.

A simulation was first made using Equations (1-3) as a baseline. A description of the input data can be found in Appendix A. The results show good agreement in the predicted and measured liquid pressures. A comparison of the input discharge coefficient, Equation (3), the calculated discharge coefficient, Equation (64), and the experimental discharge coefficient determined by Coffee is presented in Figure 3.

$$C_D = \frac{V_3}{\sqrt{2\,(P_L - P_C)/\rho_L}} \qquad (64)$$

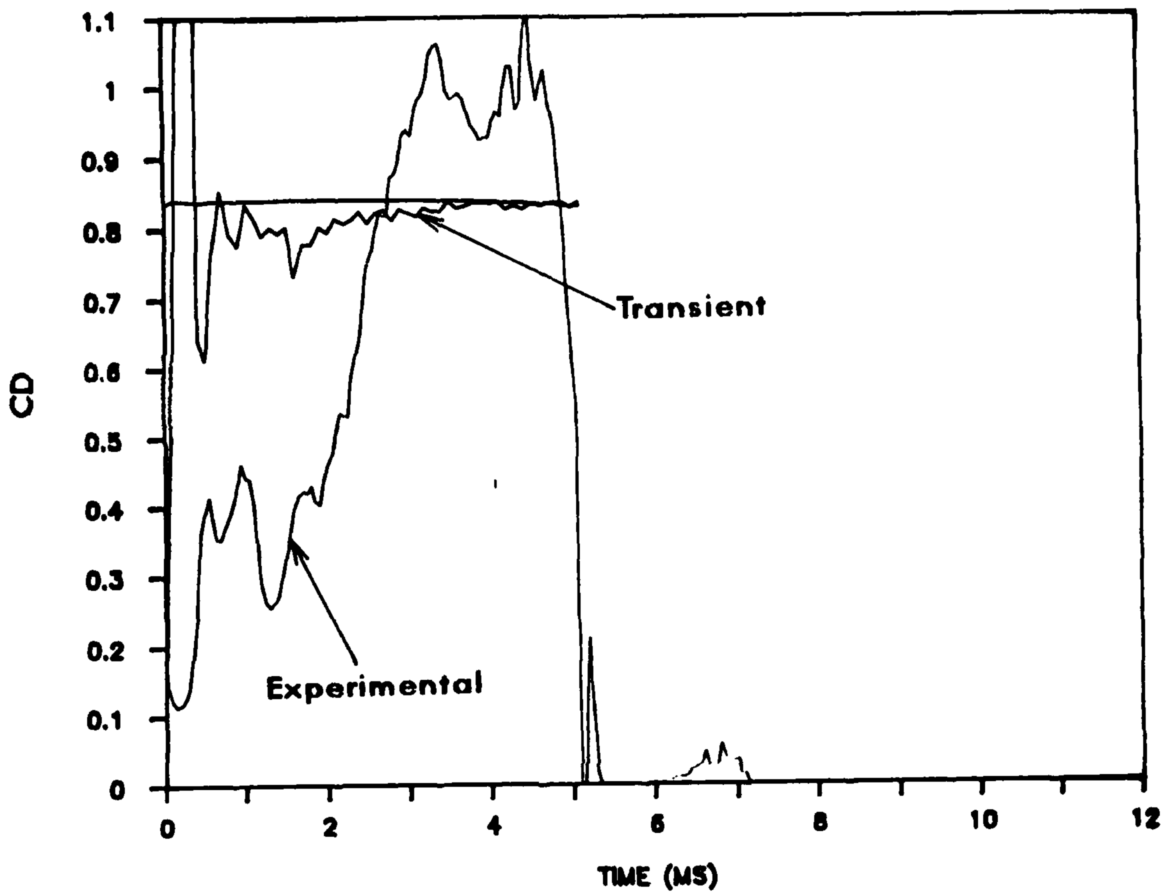

Figure 3. Discharge Coefficients from a Simplified Flow Model Without Inertial Terms

The steady state discharge coefficient is calculated from Equation (3). It varies slightly due to the variation in Reynolds Number over the ballistic cycle, but this variation is quite small.

The predicted discharge coefficient initially exhibits large oscillations, which are rapidly damped. These oscillations are a direct reflection of the hydraulic oscillations in the propellant, and the fact that the liquid flow in the orifice cannot adjust to the rapid fluctuations in liquid pressure. The result is an artificially large (and totally ficticious) "discharge coefficient" calculated from Equation (64). After the oscillations damp out at about 1.5 ms, the predicted discharge coefficient rises slowly, reaching the steady state value at about 3.5 ms as the pressures reach the steady state operating regime near maximum pressure. The "rise" in the predicted discharge coefficient coincides with the rapid rise in chamber and liquid pressures, and the acceleration of the piston to its steady state velocity. This indicates that even in the simple model, the liquid velocity lags the pressure drop from the reservoir to the chamber, resulting in an apparent "low" value for the discharge coefficient.

The experimentally determined discharge coefficient is quite different in magnitude from the predicted, but displays some general similarities. The early oscillations are present, though of a different frequency, and reduced both in magnitude and mean value. The increase in the experimental discharge coefficient to its maximum value occurs over the same interval as in the predicted case. However, the experimental discharge coefficient begins at a much lower value than predicted, about .04 ms, and peaks at about 1.1. The mean value of the experimental discharge coefficient over the steady state interval, 3.0 to 5.0 ms, is about 0.95, in comparison to a predicted value of about 0.85. Thus the simple lumped parameter simulation is not only unable to reproduce the transient behavior of the discharge coefficient, but is also unable to account for the high mean values of the experimental discharge coefficient.

The effects on the predicted discharge coefficient of extending the control volume to include the entire propellant reservoir are shown in Fig. 4. The experimental discharge coefficient, the predicted discharge coefficient using Equations (1) and (2), and the predicted discharge coefficient from the model developed here are presented. The two predicted discharge coefficients are very similar in structure. Both show the large oscillations discussed above, and both display the slow increase as the systems approaches steady state operation. However, the magnitude of the discharge coefficient obtained using our model is significantly higher than that for the simpler model. Our predicted discharge coefficient agrees quite well with the mean value of the experimentally derived data in the region of steady state operation. The lack of agreement in the early values of the discharge coefficient, and the rise to steady state is not apparent. However, it appears that there is some uncertainty in the actual piston position, which could significantly affect the computed injection area, and thus the experimental discharge coefficient. We discuss the uncertainity in the initial piston position in greater detail below.

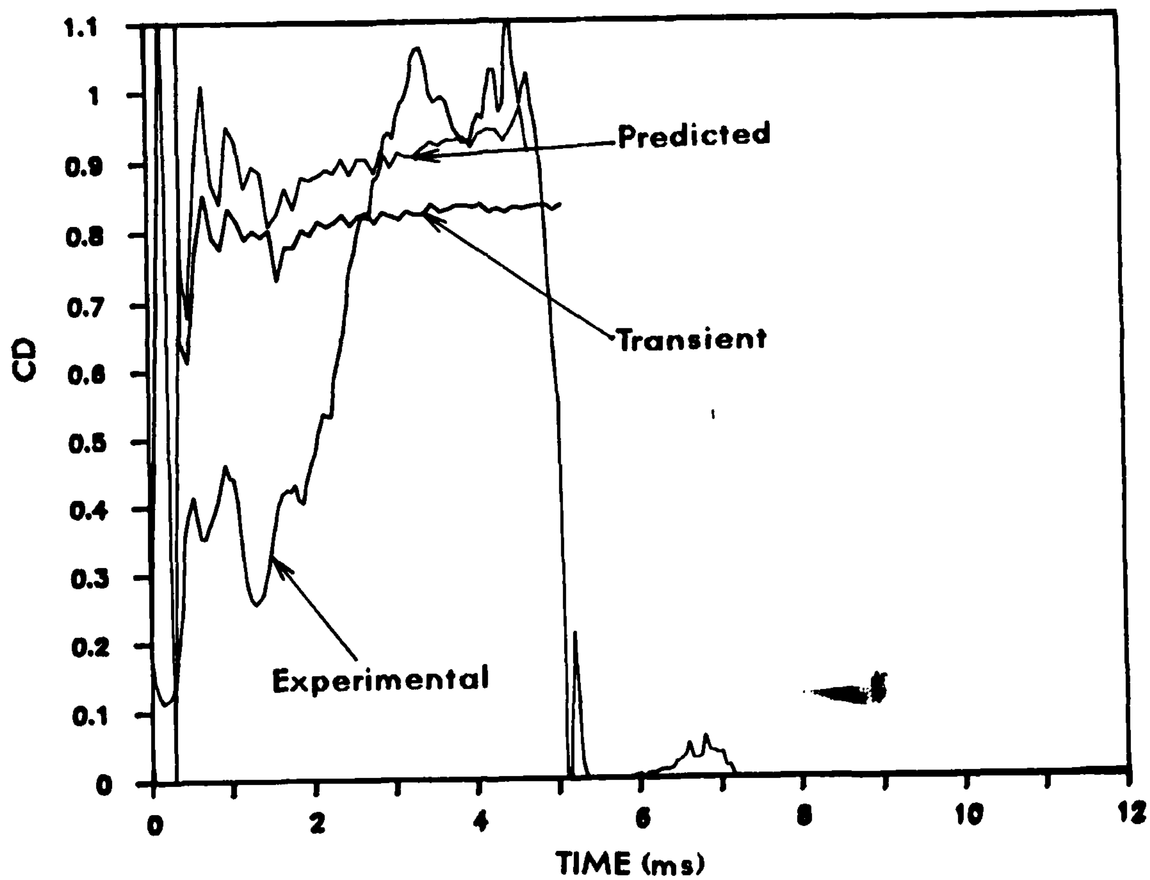

Figure 4. Discharge Coefficients from Model, Gough Formulation, and Experiment

The predicted and experimental liquid pressures and piston displacements are presented in Figs. 5 and 6 respectively. The predicted and experimental liquid pressures agree quite well over most of the ballistic cycle, however, the predicted pressure exceeds the experimental value by about 10% at peak pressure. There is an obvious discrepancy in the predicted piston motion. The experimental data indicate that the piston comes to a stop when the transducer block completes its motion, and briefly remains motionless before again accelerating. In comparison, the predicted piston motion is only slightly perturbed, and the piston continues to move with little hesitation.

In the case of the initial piston motion, the predicted, hydraulic pressure oscillations are damped more rapidly than in the experimental data. There is some uncertainty in the actual displacement of the transducer block and thus the piston. The piston is very close to the position where the injection area opens when the transducer block completes its stroke. Therefore, a slight discrepancy in the piston position can have a large effect on the injection area and thus system damping. The comparison of simulated and experimental data would suggest that the initial piston position assumed in the simulation is incorrect, and that the injector is opened too early in the process. As a result, the piston completes its stroke earlier in the simulation than in the actual experiment.

In the case of the maximum liquid pressure, the discrepancy is related to the problem with the piston motion. In the experimental data, the piston reaches the rear taper after P_{MAX}, and the chamber pressure shows an almost immediate drop as the injection area begins to decrease. However, in the simulation, the piston reaches the rear taper near P_{MAX}, as the experimental chamber pressure, which is an input, is still increasing. The combination of a decreasing injection area and an increasing chamber pressure would be an increase in liquid pressure.

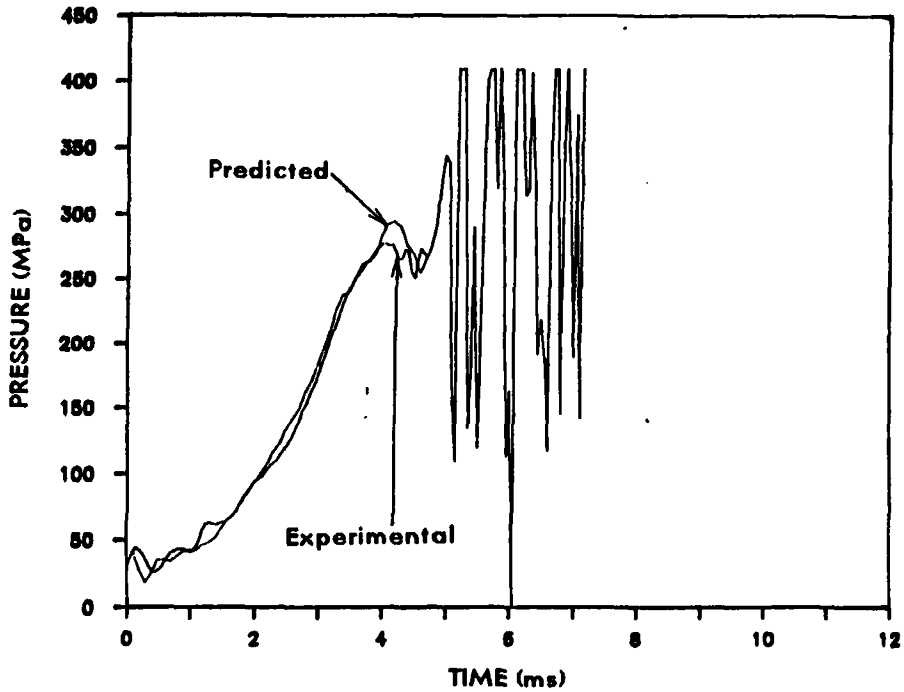

Figure 5. Predicted and Experimental Liquid Pressures

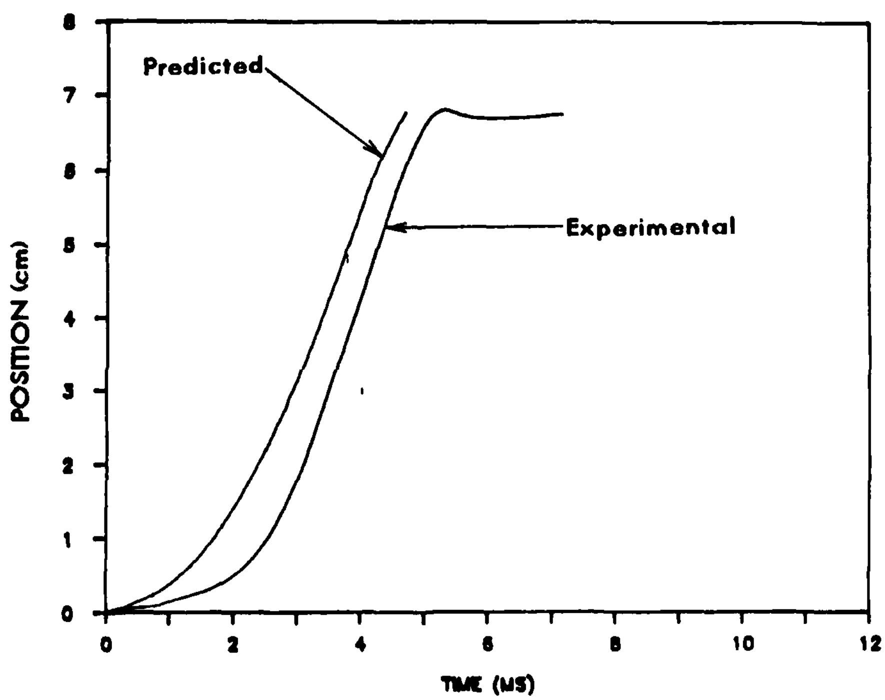

Figure 6. Predicted and Experimental Piston Position

IX. CONCLUSION

A lumped parameter model for the motion of the regenerative piston and the injection of liquid propellant has been presented. This model includes the entire propellant reservoir, and thus the effect of the inertia of the propellant in the reservoir on the process. The coupling between piston motion and liquid injection are fully included as well.

The results of computer simulations using this model are compared both with a somewhat simpler model and with data derived from experimental gun firings. The results of these comparisons are:

1. The simpler lumped parameter model exhibits a transient behavior similar to that of the experimental data, but the magnitude of the discharge coefficient is incorrect.

2. The early oscillations are related to hydraulically induced pressure oscillations in the propellant reservoir, and do not represent a real variation in the discharge coefficient.

3. The slow rise in the discharge coefficient from 3.0 ms to 5.0 ms corresponds to the period of rapid piston acceleration and rapid pressure rise. During this period, the discharge coefficient remains somewhat below the steady state value. This appears to be due to the injection velocity lagging the pressure drop during the rapid approach to steady state.

4. The maximum value of the magnitude of the discharge coefficient obtained from the simpler model is significantly less than the mean value of the experimental data. The cause of this discrepancy is not apparent.

5. The discharge coefficient obtained from a simulation using the model developed here exhibits transient behavior almost identical to that for the simpler model. However, the magnitude of discharge coefficient is significantly higher than in the case of the simpler model, and agrees quite well with the mean value of the experimental data in the steady state region.

6. There are discrepancies between the experimental liquid pressure and piston motion and the simulation using the model presented here. It appears that these discrepancies are the result of uncertainties in the initial piston position.

The next objective in this study is correction of the discrepancies. Future work will focus on the elimination of simplifying assumptions involving the system geometry, and the investigation of a more advanced RLPG configuration in which the Belleville springs are eliminated. The Lagrange pressure distribution will be extended to include the injection orifice, and the resulting pressure and velocity distributions will be compared with the results of one and two dimensional simulations.

REFERENCES

1. Gough, P.S., "Review of GE Model of Regenerative Liquid Propellant Gun," Interim Report on Work Performed Under Retainer Agreement F13-59-11651, April 1977.

2. Gough, P.S., "A Model of the Interior Ballistics of Hybrid Liquid Propellant Guns," Final Report, Contract DAAK11-82-C-0154, PGA-TR-83-4, September 1983.

3. Coffee, T., "A Lumped Parameter Code for Regenerative Liquid Propellant Guns," Technical Report BRL-TR-2703, December 1985.

4. Cushman, P.G., "Regenerative Liquid Propellant Gun Simulation User's Manual," GE Report 84-POD-004, December 1983.

5. Bulman, M.J., General Electric Ordnance Systems Division, private communication.

6. Kaufmann, W., Fluid Mechanics, McGraw-Hill, New York, 1963.

7. Pate, R.A. and Schlermen, C.P., "Flow Properties of LGP 1846 at Reduced Temperatures," Proceedings of the 22nd JANNAF Combustion Meeting, October 1985.

8. Coffee, T., "The Analysis of Experimental Measurements on Liquid Regenerative Guns," Proceedings of the 22nd JANNAF Combustion Meeting, October 1985.

9. Rizk, M.A. and Edelman, R.B., "Analysis of Transient, Multiphase Reacting Flow for Advanced LP Gun Concepts," ARO Contract No. DAAG29-83-C-0029, September 1986.

LIST OF SYMBOLS

A_3	Cross-sectional area of the vent, cm^2
A_L	Cross-sectional area of the liquid, cm^2
A_p	Cross-sectional are of the piston on chamber side, cm^2
A_R	Cross-sectional are of the piston on reservoir side, cm^2
C_D	Discharge coefficient for the liquid into the chamber
D_H	Diameter of the hole, cm
h_f	Friction loss of the liquid in the vent
h_f'	Entrance loss of the liquid into the vent
K_1	Bulk modulus at zero pressure, MPa
K_2	Derivative of bulk modulus, MPa
l_{01}	Length of the liquid column from s_0 to s_1, cm
l_{03}	Length of the liquid column from s_0 to s_3, cm
l_{12}	Length of the liquid column from s_1 to s_2, cm
l_{13}	Length of the liquid column from s_1 to s_3, cm
l_H	Length of the vent
M_p	Mass of the piston
$\dot{m}_L$	Mass flux of liquid into the combustion chamber, gm/s
P_0	Breech pressure, MPa
P_3	Combustion chamber pressure, MPa
P_L	Liquid reservoir pressure, MPa
$\bar{P}$	Space-mean pressure in the reservoir, MPa
r_1	Radius of the bolt at x_1, cm
r_2	Radius of the bolt at x_2, cm
r_b	Radius of the bolt at x, cm
R_1	Radius of the piston at s_1, cm
R_2	Radius of the piston at s_2, cm

LIST OF SYMBOLS (CON'T)

Re	Reynold's number
u_p	Velocity of the piston, cm/s
$\dot{u}_p$	Acceleration of the piston, cm/s^2
v_3	Velocity of the liquid at s_3, cm/s
$\dot{v}_3$	Acceleration of the liquid at s_3, cm/s^2
V_{12}	Volume of liquid from s_1 to s_2, cm^3
V_R	Volume of the liquid reservoir, cm^3
x_p	Position of the piston, cm
ρ_0	Density of the liquid initially, gm/cm
ρ_L	Density of the liquid at a given time, gm/cm
ψ	Discharge coefficient for the short hole

APPENDIX A

INPUT DATA FOR SIMULATION

TABLE A-1. Input Data for Simulation

RLPLCH--ROUND 8--30MM

COMBUSTION CHAMBER AREA	=	44.84700
PISTON AREA--C CH SIDE	=	34.32600
PISTON AREA--RES SIDE	=	23.27800
LENGTH L PRIME	=	1.43200
LENGTH OF VENT	=	1.04000
PISTON MASS	=	2109.20000
VOLUME LIQUID	=	172.63196
VENT OPTION	=	2
STRAIGHT LENGTH OF PIST	=	5.94680
MAX PISTON TRAVEL	=	7.37880
DENSITY LIQUID	=	1.43700
K1	=	5661.10000
K2	=	9.26490
INLET LOSS	=	0.62000
FRICTION LOSS OPTION	=	1
FRICTION LOSS	=	0.00000

TIME-C CH PRES DATA FILE: A:PTOFF64.DAT

GEOMETRY DATA FILE: A:OFF544Z.DAT

GRAPH DATA FILE: A:OF544IW.GRA

INITIAL PR IN RESERVOIR	=	29.00000
INITIAL VEL IN VENT	=	0.00000
INITIAL PISTON VELOCITY	=	358.00000
INITIAL PISTON POSITION	=	0.00000
INTEGRATOR--TINC	=	0.00010
INTEGRATOR--EPS	=	0.00001
INTEGRATOR--METH	=	1
INTEGRATOR--MITER	=	0
INTEGRATOR--KWRITE	=	0

DIFFERENTIAL EQUATION SET: 1

RAD PIST3 = 1.83000 RAD PIST2 = 1.83000 RAD PIST1 = 3.28000
RAD BOLT1 = 1.65000
VOL FUEL12= 17.90837
VOL FUEL23= 2.02661

IWRITE = 0

DISTRIBUTION LIST

No. of Copies	Organization
12	Commander Defense Technical Info Center ATTN: DTIC-DDA Cameron Station Alexandria, VA 22304-6145
1	Director Defense Advanced Research Projects Agency ATTN: H. Fair 1400 Wilson Boulevard Arlington, VA 22209
1	HQDA DAMA-ART-M Washington, DC 20310
1	Commander US Army Materiel Command ATTN: AMCDRA-ST 5001 Eisenhower Avenue Alexandria, VA 22333-0001
13	Commander Armament R&D Center US Army AMCCOM ATTN: SMCAR-TSS SMCAR-TDC SMCAR-SCA, B. Brodman R. Yalamanchili SMCAR-AEE-B, D. Downs A. Beardell SMCAR-LCE, N. Slagg SMCAR-LCS, W. Quine A. Bracuti J. Lannon SMCAR-FSS-A, R. Price L. Frauen SMCAR-FSA-S, H. Liberman Picatinny Arsenal, NJ 07806-5000
3	Director Benet Weapons Laboratory Armament R&D Center US Army AMCCOM ATTN: SMCAR-LCB-TL E. Conroy A. Graham Watervliet, NY 12189
1	Commander US Army Armament, Munitions and Chemical Command ATTN: SMCAR-ESP-L Rock Island, IL 61299-7300
1	Commander US Army Aviation Research and Development Command ATTN: AMSAV-E 4300 Goodfellow Blvd. St. Louis, MO 63120
1	Commander Materials Technology Lab US Army Laboratory Cmd ATTN: SLCMT-MCM-SB M. Levy Watertown, MA 02172-0001
1	Director US Army Air Mobility Rsch. and Development Lab. Ames Research Center Moffett Field, CA 94035
1	Commander US Army Communications Electronics Command ATTN: AMSEL-ED Fort Monmouth, NJ 07703
1	Commander ERADCOM Technical Library ATTN: STET-L Ft. Monmouth, NJ 07703-5301

DISTRIBUTION LIST

No. of Copies	Organization
1	Commander US Army Harry Diamond Labs ATTN: DELHD-TA-L 2800 Powder Mill Rd Adelphi, MD 20783
1	Commander US Army Missile Command Rsch, Dev, & Engr Ctr ATTN: AMSMI-RD Redstone Arsenal, AL 35898
1	Commander US Army Missile & Space Intelligence Center ATTN: AIAMS-YDL Redstone Arsenal, AL 35898-5500
1	Commander US Army Belvoir R&D Ctr ATTN: STRBE-WC Tech Library (Vault) B-315 Fort Belvoir, VA 22060-5606
1	Commander US Army Tank Automotive Cmd ATTN: AMSTA-TSL Warren, MI 48397-5000
1	Commander US Army Research Office ATTN: Tech Library P.O. Box 12211 Research Triangle Park,NC 27709-2211
1	Director US Army TRADOC Systems Analysis Activity ATTN: ATAA-SL White Sands Missile Range NM 88002
1	Commandant US Army Infantry School ATTN: ATSH-CD-CSO-OR Fort Benning, GA 31905

No. of Copies	Organization
1	Commander Armament Rsch & Dev Ctr US Army Armament, Munitions and Chemical Command ATTN: SMCAR-CCS-C, T Hung Picatinny Arsenal, NJ 07806-5000
1	Commandant US Army Field Artillery School ATTN: ATSF-CMW Ft Sill, OK 73503
1	Commandant US Army Armor Center ATTN: ATSB-CD-MLD Ft Knox, KY 40121
1	Commander US Army Development and Employment Agency ATTN: MODE-TED-SAB Fort Lewis, WA 98433
1	Commander Naval Surface Weapons Center ATTN: D.A. Wilson, Code G31 Dahlgren, VA 22448-5000
1	Commander Naval Surface Weapons Center ATTN: Code G33, J. East Dahlgren, VA 22448-5000
2	Commander US Naval Surface Weapons Ctr. ATTN: O. Dengel K. Thorsted Silver Spring, MD 20902-5000
1	Commander Naval Weapons Center China Lake, CA 93555-6001
1	Commander Naval Ordnance Station ATTN: C. Dale Code 5251 Indian Head, MD 20640

DISTRIBUTION LIST

No. of Copies	Organization
1	Superintendent Naval Postgraduate School Dept of Mechanical Eng. ATTN: Code 1424, Library Monterey, CA 93943
1	AFWL/SUL Kirtland AFB, NW 87117
1	Air Force Armament Lab ATTN: AFATL/DLODL Eglin, AFB, FL 32542-5000
1	AFOSR/NA (L. Caveny) Bldg. 410 Bolling AFB, DC 20332
1	Commandant USAFAS ATTN: ATSF-TSM-CN Ft Sill, OK 73503-5600
1	US Bureau of Mines ATTN: R.A. Watson 4800 Forbes Street Pittsburgh, PA 15213
1	Director Jet Propulsion Lab ATTN: Tech Libr 4800 Oak Grove Drive Pasadena, CA 91109
2	Director National Aeronautics and Space Administration ATTN: MS-603, Tech Lib MS-86, Dr. Povinelli 21000 Brookpark Road Lewis Research Center Cleveland, OH 44135
1	Director National Aeronautics and Space Administration Manned Spacecraft Center Houston, TX 77058
10	Central Intelligence Agency Office of Central Reference Dissemination Branch Room GE-47 HQS Washington, DC 20502
1	Central Intelligence Agency ATTN: Joseph E. Backofen HQ Room 5F22 Washington, DC 20505
4	Bell Aerospace Textron ATTN: F. Boorady K. Berman A.J. Friona J. Rockenfeller Post Office Box One Buffalo, NY 14240
1	Calspan Corporation ATTN: Tech Library P.O. Box 400 Buffalo, NY 14225
7	General Electric Ord. Sys Dpt ATTN: J. Mandzy, OP43-220 R.E. Mayer H. West M. Bulman R. Pate I. Magoon J. Scudiere 100 Plastics Avenue Pittsfield, MA 01201-3698
1	General Electric Company Armanent Systems Department ATTN: D. Maher Burlington, VT 05401
1	IITRI ATTN: Library 10 W. 35th St. Chicago, IL 60616
1	Olin Chemicals Research ATTN: David Gavin P.O. Box 586 Chesire, CT 06410-0586

DISTRIBUTION LIST

No. of Copies	Organization
2	Olin Corporation ATTN: Victor A. Corso Dr. Ronald L. Dotson P.O. Box 30-9644 New Haven, CT 06536
1	Paul Gough Associates ATTN: Paul Gough PO Box 1614 Portsmouth, NH 03801
1	Safety Consulting Engr ATTN: Mr. C. James Dahn 5240 Pearl St. Rosemont, IL 60018
1	Science Applications, Inc. ATTN: R. Edelman 23146 Cumorah Crest Woodland Hills, CA 91364
1	Sunstrand Aviation Operations ATTN: Dr. Owen Briles P.O. Box 7002 Rockford, IL 61125
1	Veritay Technology, Inc. ATTN: E. B. Fisher 4845 Millersport Highway, P.O. Box 305 East Amherst, NY 14051-0305
1	Director Applied Physics Laboratory The Johns Hopkins Univ. Johns Hopkins Road Laurel, Md 20707
2	Director Chemical Propulsion Info Agency The Johns Hopkins Univ. ATTN: T. Christian Tech Lib Johns Hopkins Road Laurel, MD 20707

No. of Copies	Organization
2	University of Delaware Department of Chemistry ATTN: Mr. James Cronin Professor Thomas Brill Newark, DE 19711
1	U. of ILLinois at Chicago ATTN: Professor Sohail Murad Dept of Chemical Eng Box 4348 Chicago, IL 60680
1	U. of Maryland at College Park ATTN: Professor Franz Kasler Department of Chemistry College Park, MD 20742
1	U. of Missouri at Columbia ATTN: Professor R. Thompson Department of Chemistry Columbia, MO 65211
1	U. of Michigan ATTN: Prof. Gerard M. Faeth Department of Aerospace Engineering Ann Arbor, MI 48109-3796
1	U. of Missouri at Columbia ATTN: Professor F. K. Ross Research Reactor Columbia, MO 65211
1	U. of Missouri at Kansas City Department of Physics ATTN: Prof. R.D. Murphy 1110 East 48th Street Kansas City, MO 64110-2499
1	Pennsylvania State University Dept. of Mechnical Eng ATTN: K. Kuo University Park, PA 16802

DISTRIBUTION LIST

No. of Copies	Organization
2	Princeton Combustion Rsch Laboratories, Inc. ATTN: N.A. Messina M. Summerfield 475 US Highway One North Monmouth Junction, NJ 08852
1	University of Arkansas Department of Chemical Engineering ATTN: J. Havens 227 Engineering Building Fayetteville, AR 72701

Aberdeen Proving Ground

Dir, USAMSAA
ATTN: AMXSY-D
AMXSY-MP, H. Cohen

Cdr, USATECOM
ATTN: AMSTE-TO-F

CDR, CRDEC, AMCCOM
ATTN: SMCCR-RSP-A
SMCCR-MU
SMCCR-SPS-IL

USER EVALUATION SHEET/CHANGE OF ADDRESS

This Laboratory undertakes a continuing effort to improve the quality of the reports it publishes. Your comments/answers to the items/questions below will aid us in our efforts.

1. BRL Report Number____________________Date of Report__________

2. Date Report Received______________________________

3. Does this report satisfy a need? (Comment on purpose, related project, or other area of interest for which the report will be used.)__________

4. How specifically, is the report being used? (Information source, design data, procedure, source of ideas, etc.)__________

5. Has the information in this report led to any quantitative savings as far as man-hours or dollars saved, operating costs avoided or efficiencies achieved, etc? If so, please elaborate.__________

6. General Comments. What do you think should be changed to improve future reports? (Indicate changes to organization, technical content, format, etc.)

CURRENT ADDRESS

Name

Organization

Address

City, State, Zip

7. If indicating a Change of Address or Address Correction, please provide the New or Correct Address in Block 6 above and the Old or Incorrect address below.

OLD ADDRESS

Name

Organization

Address

City, State, Zip

(Remove this sheet, fold as indicated, staple or tape closed, and mail.)

— — — — — — — — — — FOLD HERE — — — — — — — — — — —

Director
US Army Ballistic Research Laboratory
ATTN: DRXBR-OD-ST
Aberdeen Proving Ground, MD 21005-5066

NO POSTAGE
NECESSARY
IF MAILED
IN THE
UNITED STATES

OFFICIAL BUSINESS
PENALTY FOR PRIVATE USE, $300

BUSINESS REPLY MAIL
FIRST CLASS PERMIT NO 12062 WASHINGTON, DC
POSTAGE WILL BE PAID BY DEPARTMENT OF THE ARMY

Director
US Army Ballistic Research Laboratory
ATTN: DRXBR-OD-ST
Aberdeen Proving Ground, MD 21005-9989

— — — — — — — — — — FOLD HERE — — — — — — — — — — —

END
DATE
FILMED
JAN
1988